BIOCHEMISTRY
including biophysical chemistry & molecular biology

Article

pubs.acs.org/biochemistry

Insights into the GTP/GDP Cycle of RabX3, a Novel GTPase from *Entamoeba histolytica* with Tandem G-Domains

Mintu Chandra,[†] Madhumita Mukherjee,[‡] Vijay Kumar Srivastava,[†] Yumiko Saito-Nakano,[§] Tomoyoshi Nozaki,[§,∥] and Sunando Datta*,[†]

[†]Department of Biological Sciences, Indian Institute of Science Education and Research Bhopal, Bhopal 462023, India
[‡]Department of Chemical Sciences, Indian Institute of Science Education and Research Bhopal, Bhopal 462023, India
[§]Department of Parasitology, National Institute of Infectious Diseases, Shinjuku-ku, Tokyo 162-8640, Japan
[∥]Graduate School of Life and Environmental Sciences, University of Tsukuba, 1-1-1 Tennodai, Tsukuba, Ibaraki 305-8572, Japan

Supporting Information

ABSTRACT: Members of the small GTPase Ras superfamily regulate a host of systems through their ability to catalyze the GTP/GDP cycle. All family members reported thus far possess a single GTPase domain with a P-loop containing a nucleoside triphosphate hydrolase fold. Here for the first time we report a novel member from *Entamoeba histolytica*, *Eh*RabX3, which harbors two GTPase domains in tandem and exhibits unique biochemical properties. A combination of biochemical and microcalorimetric studies revealed that *Eh*RabX3 binds to a single guanine nucleotide through its N-terminal domain. Unlike most of the members of the Ras superfamily, the dissociation of the nucleotide from *Eh*RabX3 is independent of Mg^{2+}, perhaps indicating a novel mechanism of nucleotide exchange by this protein. We found that *Eh*RabX3 is extremely sluggish in hydrolyzing GTP, and that could be attributed to its atypical nucleotide binding pocket. It harbors substitutions at two positions that confer oncogenicity to Ras because of impaired GTP hydrolysis. Engineering these residues into the conserved counterparts enhanced their GTPase activity by at least 20-fold. In contrast to most of the members of the Ras superfamily, *Eh*RabX3 lacks the prenylation motif. Using indirect immunofluorescence and biochemical fractionation, we demonstrated that the protein is distributed all over the cytosol in amoebic trophozoites. Collectively, this unique ancient GTPase exhibits a striking evolutionary divergence from the other members of the superfamily.

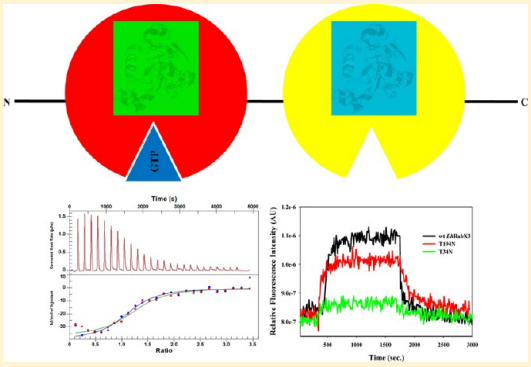

Ras superfamily GTPases act as binary molecular switches that utilize the conformational changes associated with the GTP/GDP cycle to elicit responses from target proteins and thereby regulate a broad spectrum of cellular processes, including cell proliferation, cytoskeletal assembly, nuclear transport, and intracellular membrane trafficking in eukaryotes.[1,2]

The parasitic protozoan *Entamoeba histolytica* is one of the health hazards in tropical countries. It causes amoebic dysentery and liver abscess in humans. Approximately 50 million cases of amebiasis and 40−100 thousand deaths are reported annually.[3] Vesicular trafficking plays an essential role in the survival and virulence of the parasite and is regulated by various Rab GTPases. More than one hundred Rab GTPases have been predicted to exist in the amoebic genome, with three-quarters of them being unique to the genus. This unique group has been designated as RabX. Some of the RabX proteins lack critical sequence motifs, and hence, their biochemical properties might deviate from those of their classical homologues.[4−6] Investigating the biochemical and cellular functions of these atypical Rab GTPases might unravel the cause of their unique association with the amoebic parasite.

*Eh*RabX3 is one of the atypical Rab GTPases that contains two GTPase domains (G-domains) in tandem. The only other proteins that contain two GTPase domains belong to the EngA or Der family. These latter proteins bind to two nucleotides with one in each domain and were reported in ribosome biogenesis.[7] The unique domain organization of *Eh*RabX3 prompted us to investigate the nucleotide binding and hydrolysis properties of this novel GTPase. The cellular localization of the GTPases plays a leading role in defining their function, and therefore, we probed the cellular localization of *Eh*RabX3 in the amoebic trophozoites.

In this study, we demonstrate through a series of *in vitro* experiments that *Eh*RabX3 binds to only one guanine nucleotide molecule through its N-terminal domain (NTD). Careful characterization of the site-directed and truncation mutants of *Eh*RabX3 led us to hypothesize that the C-terminal domain (CTD) plays an indispensible role in binding of the nucleotide to the NTD. *Eh*RabX3 displayed a very unusual

Received: October 21, 2013
Revised: January 28, 2014
Published: January 28, 2014

   dx.doi.org/10.1021/bi401428f | *Biochemistry* 2014, 53, 1191−1205

amino acid distribution in multiple peptide motifs associated with GTP binding or hydrolysis and consequently exhibited unique nucleotide exchange and hydrolysis properties. We showed that *Eh*RabX3 binds to a guanine nucleotide with micromolar affinity, and the binding is unaltered by Mg^{2+} ion, perhaps indicating a disparate mode of protein−nucleotide interaction. *In vitro*, *Eh*RabX3 showed an extremely sluggish GTPase activity that could be enhanced up to 15−20-fold upon introduction of site-specific mutations based on the already established mechanism of GTP hydrolysis.[8−10] Finally, the expression profile of *Eh*RabX3 in an amoebic vector showed the soluble nature of this unique GTPase.

EXPERIMENTAL PROCEDURES

Materials. Nucleotides (GDP and GTP) were purchased from Roche Molecular Biochemicals. MANT nucleotides were purchased from Molecular Probes, Life Technology. Regular molecular biology chemicals were from Sigma, and the water used for HPLC analysis was purchased from Merck. The radioactive nucleotides, [α-^{32}P]GTP and [γ-^{32}P]GTP, were obtained from BRIT (Board of Radiation and Isotope Technology, Hyderabad, India).

***Entamoeba* Culture.** Trophozoites of *E. histolytica* isolate HM-1:IMSS cl6[11] were cultured axenically in BI-S-33 medium at 35 °C as described previously.[12]

Cloning and Construction of HA-Tagged *Eh*RabX3 Plasmid To Produce Transgenic Amoeba Lines. The *E. histolytica* RabX3 cDNA sequence (GenBank accession number AB197075) was amplified via polymerase chain reaction (PCR) from the cDNA library. Primers 5′-GCC CCC GGG ATG ATT CGA CCA GCA CAT AAA TCA-3′ and 5′-CAA CTC GAG TTA CTC ATA TGA TTG TTC AAT CTT-3′ with SmaI and XhoI restriction sites, respectively, were used for PCR amplification. The PCR product (1050 bp) was purified and cloned into the SmaI and XhoI sites of the p*Eh*ExHA vector[13] containing a HA tag at the N-terminus (HA-*Eh*RabX3).

Subcloning of *Eh*RabX3 into the Bacterial Expression Vector. DNA fragments containing the *Eh*RabX3 gene were amplified from the p*Eh*ExHA vector by PCR and subsequently subcloned into bacterial cloning vector pT7blue and pET28a (Novagen) between BamHI and XhoI restriction sites. The N-terminal (amino acids 1−176, designated *Eh*RabX3a) and C-terminal (amino acids 177−349, *Eh*RabX3b) domains (http://www.pfam.sanger.ac.uk/) were amplified using a pair of primers (Table 1 of the Supporting Information) and further subcloned into the pET28a vector as well as the pGEX6p1 vector between EcoRI and HindIII restriction sites.

Site-Directed Mutagenesis. A PCR-based method (Quikchange mutation kit, Stratagene) was used to generate the different *Eh*RabX3 mutants (T34N, T194N, V71A, K73Q, and V71A/K73Q) using a plasmid encoding wild-type *Eh*RabX3 as the template. A pair of oligonucleotide primers (Table 1 of the Supporting Information) containing the desired mutation were used for the PCRs. The template plasmid DNA was linearized by DpnI digestion before transformation into *Escherichia coli* strain DH5α. Mutations were verified by DNA sequence analysis.

Protein Expression and Purification. To express the recombinant proteins, appropriate plasmids were transformed into *Es. coli* BL21(DE3) cells. Overnight cultures were grown at 37 °C. The freshly inoculated bacterial cells were grown at 37 °C until the OD_{600} reached 0.6, and the temperature was reduced from 37 to 20 °C before overnight induction with 100 μM isopropyl β-D-thiogalactoside (IPTG). Cells were harvested by centrifugation at 4 °C; the bacterial pellet was dissolved in lysis buffer containing 50 mM Tris (pH 8.0), 300 mM NaCl, 5 mM 2-mercaptoethanol, 1% Triton X-100, 5 mM $MgCl_2$, 10 μg/mL protease inhibitor cocktail, 200 μM phenylmethanesulfonyl fluoride (PMSF), and 100 μM GDP and the cells were lysed with a sonicator (Branson). After sonication, cell debris were removed by centrifugation at 30000*g*, and the supernatant was loaded onto a column containing Ni-NTA metal affinity resins (GE Healthcare) for six-His-tagged proteins, glutathione sepharose resin (GE Healthcare) for GST-tagged proteins, and amylose resin (GE Healthcare) for MBP-tagged proteins, according to the manufacturer's protocols. The column was thoroughly washed with lysis buffer containing 100−500 mM salt. Finally, the protein of interest was eluted with a linear gradient of imidazole (from 100 to 250 mM) in 50 mM Tris (pH 8.0) and 300 mM NaCl; the GST-tagged protein was eluted with 10 mM reduced glutathione in 50 mM Tris (pH 8.0) and 300 mM NaCl, and the MBP-tagged protein was eluted with 10 mM maltose in 50 mM Tris (pH 8.0) and 300 mM NaCl. Fractions containing the desired protein, as revealed by sodium dodecyl sulfate−polyacrylamide gel electrophoresis (SDS−PAGE) and Western blotting, were pooled and dialyzed against gel filtration buffer [50 mM Tris (pH 8.0), 50 mM NaCl, 5 mM $MgCl_2$, 5 mM dithiothreitol (DTT), and 7% glycerol]. For further purification, the dialyzed protein was injected into a Superdex 75 prep grade (16/60) gel filtration column (GE Healthcare), equilibrated with the same buffer. Fractions containing pure protein, as revealed by SDS−PAGE, were pooled and concentrated using a 10 kDa cutoff concentrator (Centricon, Millipore) to 10 mg/mL and stored at −80 °C.

Preparation of Metal Ion- and Nucleotide-Free Apo-*Eh*RabX3. To prepare the nucleotide-free form of *Eh*RabX3, the purified protein samples (~100 μM) were incubated in buffer containing 50 mM HEPES (pH 7.3) and 20 mM EDTA for 20 min at 25 °C, followed by centrifugation in a Centricon 10 kDa concentrator at 4000*g* until the protein concentration had been enhanced approximately 7−10-fold. The steps described above were repeated three more times, and the samples were subsequently exchanged into buffer containing 50 mM HEPES (pH 7.3), 100 mM NaCl, and 1 mM DTT until the concentration reached 100 μM.[14] To examine the content of the nucleotide remaining in the protein samples, an aliquot (100 μL) of the sample was taken, denatured by being boiled, and injected into the HPLC system. The HPLC profile showed that the sample was approximately 85−90% devoid of nucleotide.

Isothermal Titration Calorimetry (ITC). ITC experiments to determine the thermodynamics of binding were conducted with a nano ITC apparatus (TA Instruments). Before the ITC experiment, traces of metal ions were removed from *Eh*RabX3 protein solution through incubation with an excess of EDTA and subsequent dialysis in HEPES buffer [25 mM HEPES (pH 7.3) and 100 mM NaCl]. In a typical experimental setup, the cell was filled with 300 μL of *Eh*RabX3 and the syringe contained a 50 μL solution of the nucleotide (GDP/GTP). All solutions were degassed prior to being loaded into the cell. Aliquots (2 μL) of 500 μM nucleotide (GDP/GTP) solutions were injected into a 50 μM *Eh*RabX3 protein solution at an interval of 3 min with the syringe rotating at 300 rpm to ensure proper mixing. The heat of dilution was measured by injecting the nucleotide (GDP/GTP) into the buffer solution and

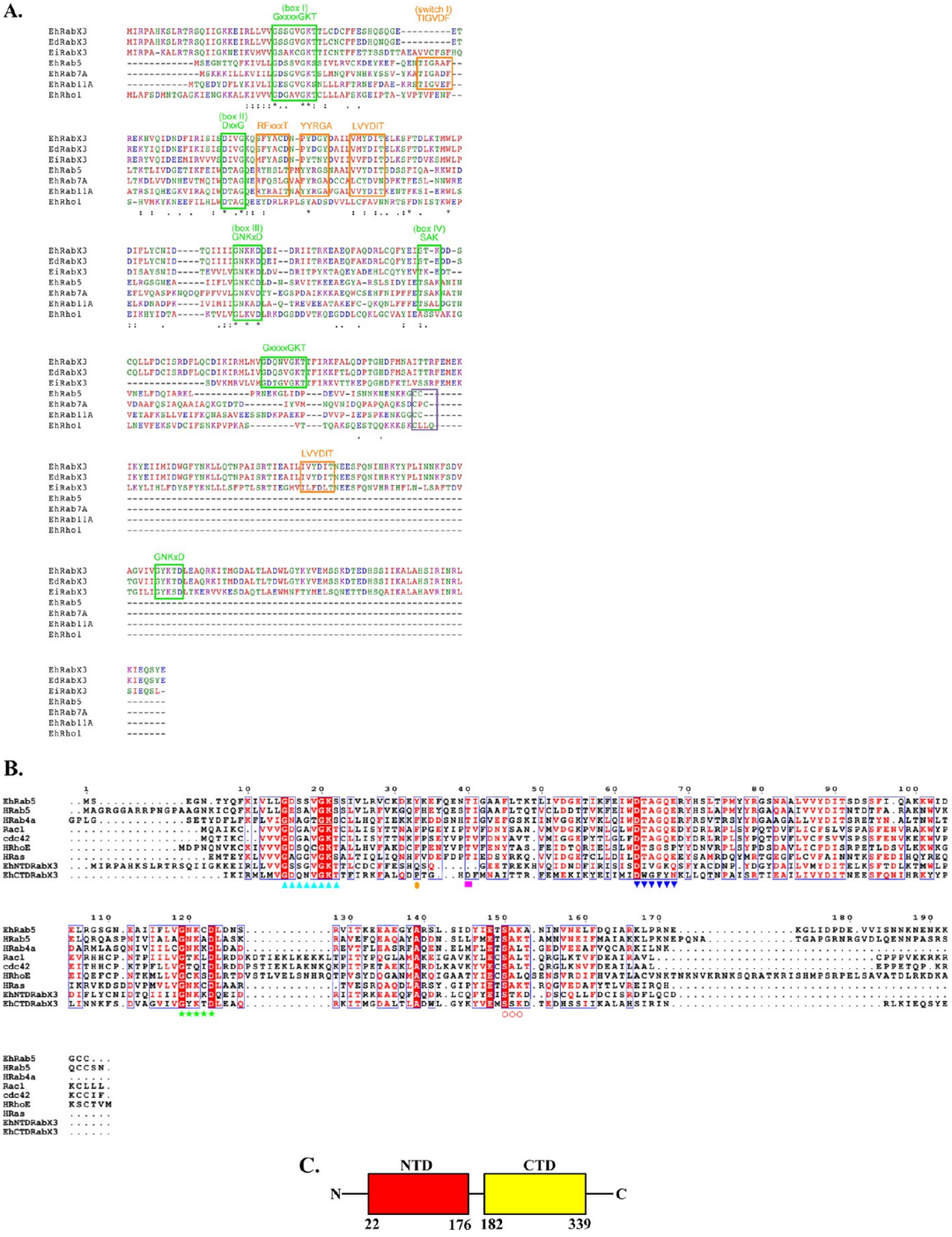

Figure 1. Sequence alignment of *Entamoeba* RabX3 homologues and conventional Rab that depicts the presence of two GTPase domains in *Eh*RabX3. (A) ClustalW was used for alignment analysis. Hydrophobic, hydrophilic, basic, and acidic residues among seven proteins are colored red, green, purple, and blue, respectively. The region involved in nucleotide binding, the Rab GTPase-specific switch I and switch II regions, and the C-terminal cysteines involved in membrane targeting are boxed in green, orange, and black, respectively. The sequences are from *Eh*RabX3 (GenBank accession number AB197075), *Entamoeba dispar* RabX3 (EDI_126470), *Entamoeba invadens* RabX3 (EIN_135850), *Eh*Rab5 (XP_655377), *Eh*Rab7A (XP_649196), *Eh*Rab11A (XP_647948), and *Eh*Rho1 (XP_654488). (B) Sequence alignment of the NTD and CTD of *Eh*RabX3 with Ras and Rho family GTPases generated using ClustalW[61] and ESPript version 2.2.[62] The P-loop-specific sequence (GXXXXGKS/T), the guanine base-stabilizing residue (F), the switch I-specific sequence (T), the switch II-specific sequence (DXXGQE), and the guanine base-recognizing sequence (GNKXD and SAK) are highlighted by different invariant colors as shown. (C) Domain architecture of *Eh*RabX3 as predicted from a Pfam database search (http://www.pfam.sanger.ac.uk/). The search revealed the presence of two Ras-like GTPase domains in *Eh*RabX3 with *e* values of 1.4×10^{-25} and 7.9×10^{-22}.

subtracted from the heat of interaction.[15] Data were analyzed using Nanoanalyser software by fitting to a one-set-of-sites model. For metal binding experiments, 2 μL aliquots of 1 mM $MgCl_2$ solutions were injected into a 100 μM protein solution. The heat of dilution was measured by injecting $MgCl_2$ into the buffer solution. The analysis yielded binding stoichiometry (n),

dx.doi.org/10.1021/bi401428f | *Biochemistry* 2014, 53, 1191−1205

binding constant (K_a), and enthalpy of binding (ΔH) values. From these values, the free energy of binding (ΔG) and the entropy of binding (ΔS) were calculated from the following thermodynamic equations:

$$\Delta G = -RT \ln K$$

and

$$\Delta G = \Delta H - T\Delta S$$

The dissociation constant (K_d) was calculated as $1/K_a$.

Fluorescence Measurements. Fluorescence measurements were performed with fluoromax-4 spectrofluorimeter (Horiba Jobin). The fluorescence of MANT-GTP was measured directly with a $\lambda_{excitation}$ of 360 nm and a $\lambda_{emission}$ of 440 nm. Experiments were performed in buffer A, which consisted of 25 mM HEPES (pH 7.3), 100 mM NaCl, and 2 mM DTT (with or without Mg^{2+}) at 25 °C. Observed association rate constants were evaluated by fitting the increase in fluorescence into an exponential rise model

$$F(t) = F_0 + A(1 - e^{-k_{obs}t})$$

while dissociation rate constants were evaluated by fitting the fluorescence change into first-order decay kinetics

$$F(t) = F_0 + Ae^{-k_{obs}t}$$

where $F(t)$ is the fluorescence at time t, k_{obs} and A are the observed rate constant and amplitude, respectively, and F_0 is the initial fluorescence.[16−19] For fluorescence emission measurements, 350 nM MANT-GTP was incubated with various concentrations of apo-*Eh*RabX3 (1, 2, and 5 μM) in the presence or absence of Mg^{2+}. After incubation for 1 h, the emission spectra (380−500 nm) were recorded.[14]

Nitrocellulose Filter Binding Assay. To determine the nucleotide binding affinities for *Eh*RabX3 and various truncated mutants, [α-^{32}P]GTP (specific activity of 3000 Ci/mmol) was incubated with the protein at 25 °C for 1.5 h in buffer A containing 5 mM $MgCl_2$. The binding reactions were stopped by adding ice-cold binding buffer A followed by filtration through nitrocellulose membranes (BA 85, 0.45 μm pore size, Schleicher & Schuell). The membranes were washed three times with 3 mL of ice-cold buffer A and allowed to dry in air. The amount of radioactive nucleotide that remained bound to the protein was quantified with a scintillation counter (Microplate counter, Microbeta^2, Perkin-Elmer).[14]

Nucleotide Analysis by HPLC. The nucleotide analyses were performed using a Sunfire C-18 reversed phase column (0.46 cm × 25 cm) filled with 5 μm (particle size) silica (Waters). The column was equilibrated with buffer containing 100 mM KH_2PO_4 (pH 6.5), 10 mM tetrabutylammonium bromide, 0.2% sodium azide (NaN_3), and 7.5% acetonitrile, and isocratic elution was performed at ambient temperature with a flow rate of 1 mL/min. In this system, the order of elution of guanine nucleotides was GDP and GTP (retention times of ∼5 and 7 min, respectively). In a typical experiment, 100 μM protein was boiled for 3 min at 100 °C and centrifuged at 13000*g* for 10 min to remove the denatured protein. An aliquot of the supernatant (20 μL) was injected into the column. The column was calibrated with 25, 50, 100, and 200 μM solutions of the different guanine nucleotides (GDP and GTP).[20,21]

Measurement of the Intrinsic GTPase Activity. The kinetics of GTP hydrolysis (P_i release) was measured under single-turnover conditions using [γ-^{32}P]GTP.[26−29] To determine the single-turnover rate of GTP hydrolysis, a total of 200 μM protein was exchanged with [γ-^{32}P]GTP (10 μCi/μL) in buffer A containing 10 mM EDTA and 2 mM unlabeled GTP at 25 °C for 1.30 h. After the exchange, the reaction mixture was loaded onto the equilibrated desalting column (NAP-5, GE Healthcare), and finally, it was eluted in 500 μL of assay buffer and collected on ice. The assay was initiated by adding 20 mM $MgCl_2$ to the eluted protein in the presence of 10 mM AMPPNP and 10 mM cold GTP. At specific time points, 15 μL aliquots were removed and added to 985 μL of a 5% charcoal solution (prepared in 50 mM NaH_2PO_4). The samples were centrifuged at 12000*g* for 4 min; 500 μL of the supernatant was carefully added to scintillation fluid and further quantified with a scintillation counter.[22−24]

Establishment of HA-Tagged *Eh*RabX3-Expressing Amoeba Cell Lines. The plasmid was introduced into the amoebic trophozoites by lipofection as previously described.[25] Transformant trophozoites were maintained under 6 μg/mL geneticin.

Indirect Immunofluorescence. The indirect immunofluorescence assay was performed as previously described[26] with some modifications. Briefly, amoeba transformant cells expressing HA-*Eh*RabX3 were transferred to 8 mm round wells on a slide glass and fixed with 3.7% paraformaldehyde in phosphate-buffered saline (PBS, pH 7.2) for 10 min. The sample was permeabilized with 0.1% Triton X-100 in PBS for 10 min and reacted with a primary antibody at a 1:500 dilution (anti-HA monoclonal antibody, 11MO, Covance, Princeton, NJ). After being washed, the samples were then incubated with Alexa Fluor 488-conjugated anti-mouse secondary antibody (1:1000) for 1 h. The samples were examined on a Carl- Zeiss LSM 510 META confocal laser scanning microscope, and images were analyzed using LSM510 software.

Subcellular Fractionation. Approximately 3 × 10^5 trophozoites were washed with cold PBS, resuspended in homogenization buffer [250 mM sucrose, 50 mM Tris (pH 7.5), 5 mM $MgCl_2$, and 0.1 mg/mL E-64], and homogenized on ice with 30 strokes by a Dounce homogenizer with a tight-fitting pestle as described previously.[27] After unbroken cells had been removed by centrifugation at 4500*g* for 2 min, the supernatant was centrifuged at 13000*g* and 4 °C for 10 min to obtain the pellet (p13) and supernatant (s13) fractions. The s13 fraction was further separated by centrifugation at 100000*g* and 4 °C for 1 h to obtain the pellet (p100) and soluble (s100) fractions. These fractions were subjected to immunoblot analyses with the anti-HA, anti-CPBF1,[28−30] or anti-ICP1[31] antibody.

RESULTS

***Eh*RabX3 Is a Novel Rab Protein with Two GTPase Domains in Tandem.** We have previously reported that the primary sequence of *Eh*RabX3 (GenBank accession number AB197075) is double the length of those of the conventional small GTPases and conserved in other *Entamoeba* species.[4,32] The amino acid sequence of the N-terminal region of *Eh*RabX3 possesses conserved nucleotide binding motifs, including Rab family-specific residues[33] (Figure 1A,B). In addition, an intact phosphate binding motif and part of the other GTPase-specific motifs were present in the C-terminal region of *Eh*RabX3 and its homologues in all other *Entamoeba* species (Figure 1A). Thus, *Eh*RabX3 is likely to have two GTPase domains, an idea further supported by Pfam-based analysis (http://www.pfam.sanger.ac.uk/) that predicted the presence of two Ras-like GTPase domains in *Eh*RabX3 with *e* values of 1.4 × 10^{-25} and

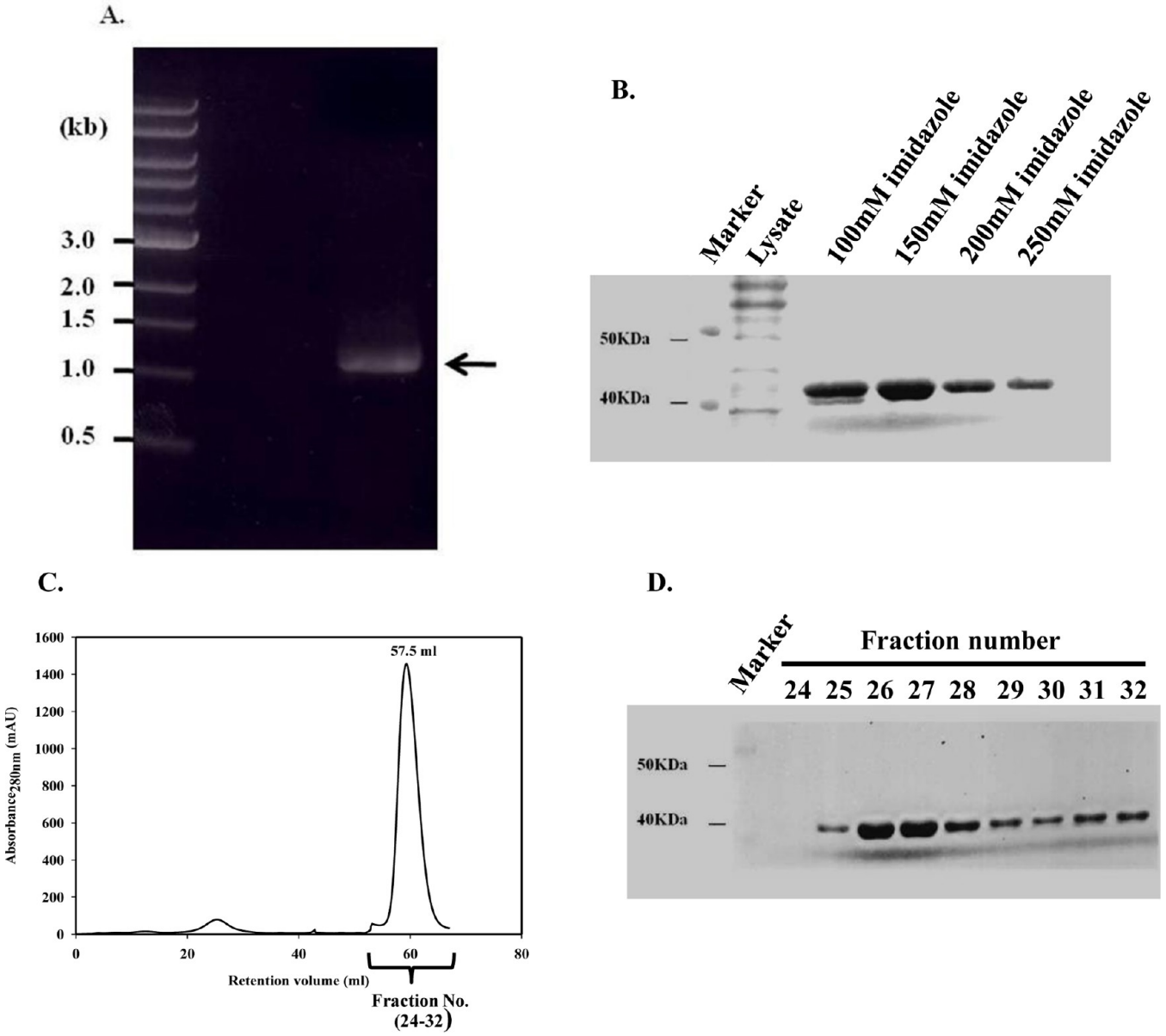

Figure 2. Cloning, expression, and purification of full-length *Eh*RabX3. (A) PCR amplification of full-length *Eh*RabX3 cDNA. Specific oligonucleotides, designed for the amplification of full-length *Eh*RabX3 cDNA, were used to amplify the single 1050 bp band as indicated by the arrowhead. (B) Affinity purification profile of six-His-tagged *Eh*RabX3. The whole cell lysate and eluted fractions (100−250 mM imidazole) from the affinity column were analyzed using SDS−PAGE. (C) Size exclusion chromatogram of *Eh*RabX3. Fractions from affinity-purified *Eh*RabX3 were pooled and subjected to a Superdex 75 prep grade gel filtration column (16/60). *Eh*RabX3 was eluted at a retention volume of 57.2 mL, which corresponds to a molecular mass of 41 kDa. (D) Fractions 24−32 corresponding to the chromatogram peaks were analyzed using SDS−PAGE.

7.9×10^{-22} (Figure 1C). Another distinct GTPase family, EngA, widely present in bacteria and higher plants,[34] also acquired two GTPase domains and is involved in ribosomal biogenesis.[35] We noticed EngA GTPase, which does not have Rab-specific sequences, is also presented in several protozoan organisms, including *Micromonas* and *Paulinella*, by the genomic database search (Figure S1 of the Supporting Information). Thus, *Eh*RabX3 is a novel Rab GTPase conserved in *Entamoeba* species.

Cloning, Expression, and Purification of Full-Length *Eh*RabX3. To investigate the biochemical properties of *Eh*RabX3, the full-length *Eh*RabX3 sequence was amplified from cDNA extracted from reference strain *E. histolytica* HM1. A single 1050 bp fragment was amplified via PCR with *Eh*RabX3-specific primers (Figure 2A). To prepare the recombinant *Eh*RabX3 protein, we subcloned its protein coding region into bacterial cloning vector pET28a. Under optimized conditions (see Experimental Procedures), *Eh*RabX3 was purified in the soluble fraction using two-step chromatography, an affinity column, and then size exclusion chromatography (Figure 2B−D).

***Eh*RabX3 Binds to One Molecule of Guanine Nucleotide through Its N-Terminal GTPase Domain.** The presence of two nucleotide binding domains inspired us to characterize guanine nucleotide (GDP/GTP) binding to *Eh*RabX3. We used isothermal titration calorimetry (ITC) to measure the stoichiometry and affinity of the guanine nucleotide (GDP/GTP) for *Eh*RabX3. Because of the presence of two binding domains, the calorimetric data obtained were analyzed using Nanoanalyser software by fitting to a "one-set-

dx.doi.org/10.1021/bi401428f | *Biochemistry* 2014, 53, 1191−1205

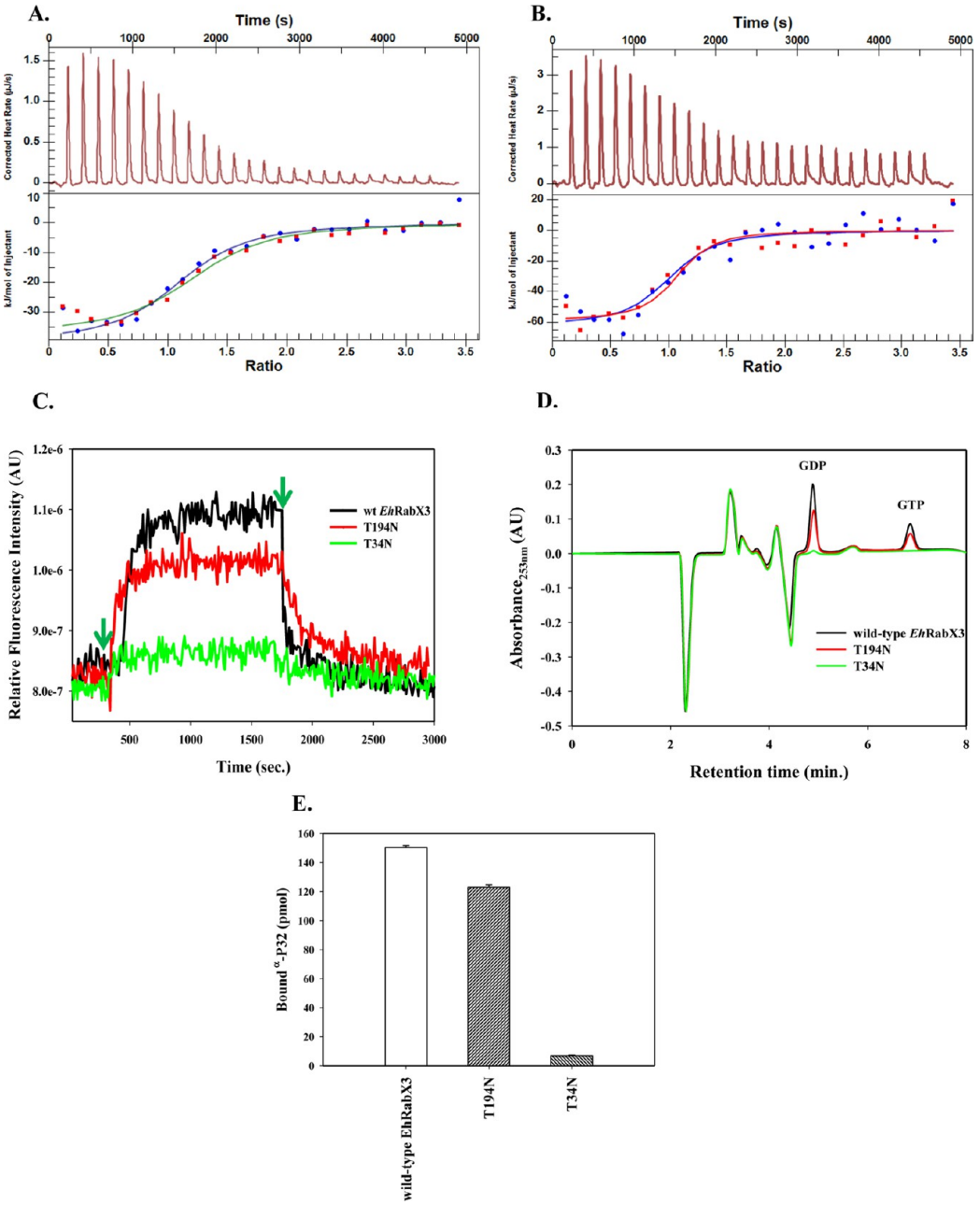

Figure 3. *Eh*RabX3 binds to a single guanine nucleotide through its N-terminal G-domain. Calorimetric titration of (A) GDP and (B) GTP with *Eh*RabX3. The top panel shows the raw ITC data obtained from 25 injections of 2 μL aliquots of 500 μM GTP into 50 μM *Eh*RabX3. The bottom panel shows the integrated heats obtained from the raw data after subtraction of the dilution enthalpy of GDP and GTP. All data were replicated and all experiments conducted at 25 °C. The dotted line shows the fitted curve obtained using the single-set-of-sites model. Experiments were conducted at 25 °C as described in Experimental Procedures. (C) Comparison of nucleotide binding to wild-type *Eh*RabX3 and the T34N and T194N mutants. After the baseline had been set with 350 nM MANT-GTP in buffer A containing 5 mM $MgCl_2$, 2 μM *Eh*RabX3, T34N, or T194N was added to MANT-GTP-containing buffer at the indicated time (marked by an arrowhead), and the enhancement of fluorescence intensity was monitored. Upon saturation, excess unlabeled GTP (200 μM) was added (marked by an arrowhead) to dissociate bound MANT-GTP from each of the recombinant proteins. (D) HPLC measurement of the nucleotide occupancy of wild-type *Eh*RabX3, T34N, and T194N. Wild-type *Eh*RabX3, T34N, or T194N (100 μM) was boiled for 3 min and centrifuged at high speed (13000*g*) for 10 min. Twenty microliters of the supernatant was injected into into the C18 reverse phase HPLC column equilibrated with 100 mM KH_2PO_4 (pH 6.5), 10 mM tetrabutylammonium bromide, 0.2% NaN_3, and 7.5% acetonitrile, and isocratic elution was performed. (E) Measurement of the binding of guanine nucleotide to wild-type *Eh*RabX3, T34N, and T194N. Each recombinant protein (2 μM) was preloaded with [α-^{32}P]GTP and incubated at 25 °C with buffer A in the presence of 200 μM GTP. After 1.5 h, 50 μL aliquots were removed from each sample and bound nucleotides were quantified by the filter binding method. The data represent the average of three independent experiments.

of-sites" model as well as a "multiple-set-of-sites" model. The thermodynamic parameters obtained by fitting to both models were then analyzed statistically with 100 trials, keeping the standard deviation at 0.1 and a desired confidence level of 99%. The data fit far better to the single-set-of-sites model[36] and gave good Gaussian distributions for the thermodynamic parameters (Figure S2 of the Supporting Information). To obtain the thermodynamic parameters, we analyzed the thermogram by a

dx.doi.org/10.1021/bi401428f | *Biochemistry* 2014, 53, 1191−1205

Table 1. Thermodynamic Parameters for Binding of *Eh*RabX3 to Guanine Nucleotides (GDP and GTP) As Determined by ITC[a]

ligand	[ligand] (mM)	[*Eh*RabX3] (μM)	ΔH (kJ mol^{-1})	ΔS (J mol^{-1} K^{-1})	K_a (M^{-1})	K_d (M)	n (ligand:*Eh*RabX3)
GDP	0.5	50	−39.6 ± 0.25	−29.1	2.7 × 10^5 ± 8.3 × 10^3	3.7 × 10^{-6}	1.1 ± 0.005
GTP	0.5	50	−62.1 ± 0.21	−99.4	4.9 × 10^5 ± 1.1 × 10^4	2.02 × 10^{-6}	0.99 ± 0.002

[a]Listed are the estimates of thermodynamic parameters (ΔH and ΔS) as well as association (K_a) and dissociation (K_d) equilibrium constants and binding stoichiometries (n) for binding of GDP and GTP to *Eh*RabX3 at 25 °C. All measurements were performed in duplicate in HEPES buffer [25 mM HEPES (pH 7.3) and 100 mM NaCl].

curve fitting procedure in which a nonlinear regression approach was used to fit the model to the data to give best values of the fitting parameters. The fitted data (Figure 3A,B) showed a 1:1 stoichiometry, indicating the binding of one molecule of GDP/GTP to one *Eh*RabX3. Table 1 shows the values of the thermodynamic parameters obtained through the nonlinear regression fitting. The constants for binding of GDP and GTP to *Eh*RabX3 are comparable. The dissociation constants reveal micromolar affinity as reported elsewhere.[37,38]

To address the question of which of the two GTPase domains is involved in the binding of the nucleotide, a site-directed point mutation approach was used. Ras superfamily small GTPases are identified by a specific set of sequence motifs.[39] Mutations in these motifs dramatically influence the guanine nucleotide binding and hydrolysis processes. We generated two point mutants, T34N and T194N, in the NTD and CTD, respectively. The point mutation at this position was well characterized and known to drastically reduce the affinity of the nucleotide for GTPases. Thus, binding of the nucleotide to T34N and T194N was assayed using the fluorescence spectroscopic readout. The data show a dramatic reduction in the nucleotide exchange activity for T34N, but an only 10−15% change was observed for T194N, suggesting that the N-terminal phosphate binding motif is essential for binding of the nucleotide to *Eh*RabX3 (Figure 3C). We further estimated the amount of protein-bound nucleotides by HPLC (Figure 3D) using the standard curve from GDP and GTP (Figure S3 of the Supporting Information). The total amount of nucleotides bound to the T34N mutant was found to be only 10 ± 2.45% (n = 3) of that of wild-type *Eh*RabX3 (Table 2). Thus, these data suggest that *Eh*RabX3 binds to the nucleotide through its NTD. The binding results were also confirmed by a radioactivity-based filter binding assay (Figure 3E).

The CTD Is Necessary for Binding of the Nucleotide to *Eh*RabX3. To address whether the C-terminal GTPase domain of *Eh*RabX3 contributes to the overall nucleotide binding to the protein, two partial constructs corresponding to N-terminal (amino acids 1−176) and C-terminal (amino acids 177−349) domains (http://www.pfam.sanger.ac.uk/) of *Eh*RabX3 were designed. Their nucleotide binding activity was assayed by a radioactivity-based filter binding assay and autoradiography. As shown in panels A and B of Figure 4, both domains show a compromised nucleotide binding ability compared to that of the full-length protein. To further delineate the minimal GTP binding region of *Eh*RabX3, four deletion mutants were generated by truncating C-terminal regions (amino acids 1−202, 1−280, 1−289, and 1−302), and their nucleotide binding ability was assayed. As shown in panels C and D of Figure 4, none of the C-terminally truncated mutants could show efficient nucleotide binding like that of *Eh*RabX3, indicating a potential role of the CTD in maintaining the structural integrity of *Eh*RabX3.

Table 2. Summary of the Nucleotide Occupancy by Wild-Type *Eh*RabX3 and Its T194N and T34N Mutants by HPLC[a]

protein	% GDP	% GTP
*Eh*RabX3	45 ± 3.45	20 ± 3.21
T194N	34 ± 2.38	14 ± 2.64
T34N	7 ± 2.51	−

[a]Listed are percentages of wild-type and mutant (T194N and T34N) *Eh*RabX3 bound to nucleotides (GTP and GDP). Each value represents the average of three independent experiments, using three different preparations of each of the recombinant proteins, and were corrected for the background obtained with the buffer alone as the blank. The bound nucleotides were quantified on the basis of HPLC analyses as shown in Figure 3D using the standard calibration curves for GDP and GTP (Figure S3 of the Supporting Information).

***Eh*RabX3 Exhibits Mg^{2+} Ion-Independent Guanine Nucleotide Exchange Activity.** Ras superfamily small GTPases are known to bind to guanine nucleotides in a Mg^{2+}-dependent manner. Addition of the divalent ion stabilizes the nucleotide in the binding pocket, whereas its removal by chelating reagents weakens the affinity for the nucleotide. To investigate whether *Eh*RabX3 behaves in a similar fashion, we set up a real-time fluorescence-based assay to measure nucleotide binding affinity for the protein in the presence and absence of Mg^{2+}. We used 2′/3′-*O*-(*N*′-methylanthraniloyl) (MANT)-conjugated nucleotides, which, when they bind to the protein, show a dramatic enhancement of the fluorescence intensity that can be reversed by adding unconjugated nucleotides as shown in Figure 5A. We further recorded emission spectra of MANT-GTP bound to *Eh*RabX3 in the absence and presence of Mg^{2+}. As shown in Figure 5B, addition of *Eh*RabX3 to MANT-GTP led to a dose-dependent increase in fluorescence emission, indicating the formation of the *Eh*RabX3−MANT-GTP complex, that remained unaltered upon addition of Mg^{2+}. The $\lambda_{emission}$ for MANT-GTP remained unaltered by the divalent cation.

To examine whether Mg^{2+} has any effect on the kinetic parameters, we carefully studied the association and dissociation kinetics of binding of the nucleotide to *Eh*RabX3 in the presence or absence of the metal ion. The dissociation rate was determined in displacement experiments in which an excess of unlabeled GTP was used to displace MANT-GTP from its complex with *Eh*RabX3. Time courses of MANT-GTP dissociation monitored by the decrease in fluorescence intensity could be fit to single exponentials (Figure 5C), giving the first-order dissociation rate constant values (Table 3). The dissociation rate was found to be unaltered by Mg^{2+}. The result described above was also verified by a radioactivity-based filter binding assay (Figure S4 of the Supporting Information). Next, we measured the kinetics of MANT-GTP association under pseudo-first-order conditions using a constant concentration of MANT-GTP and increasing concentrations of

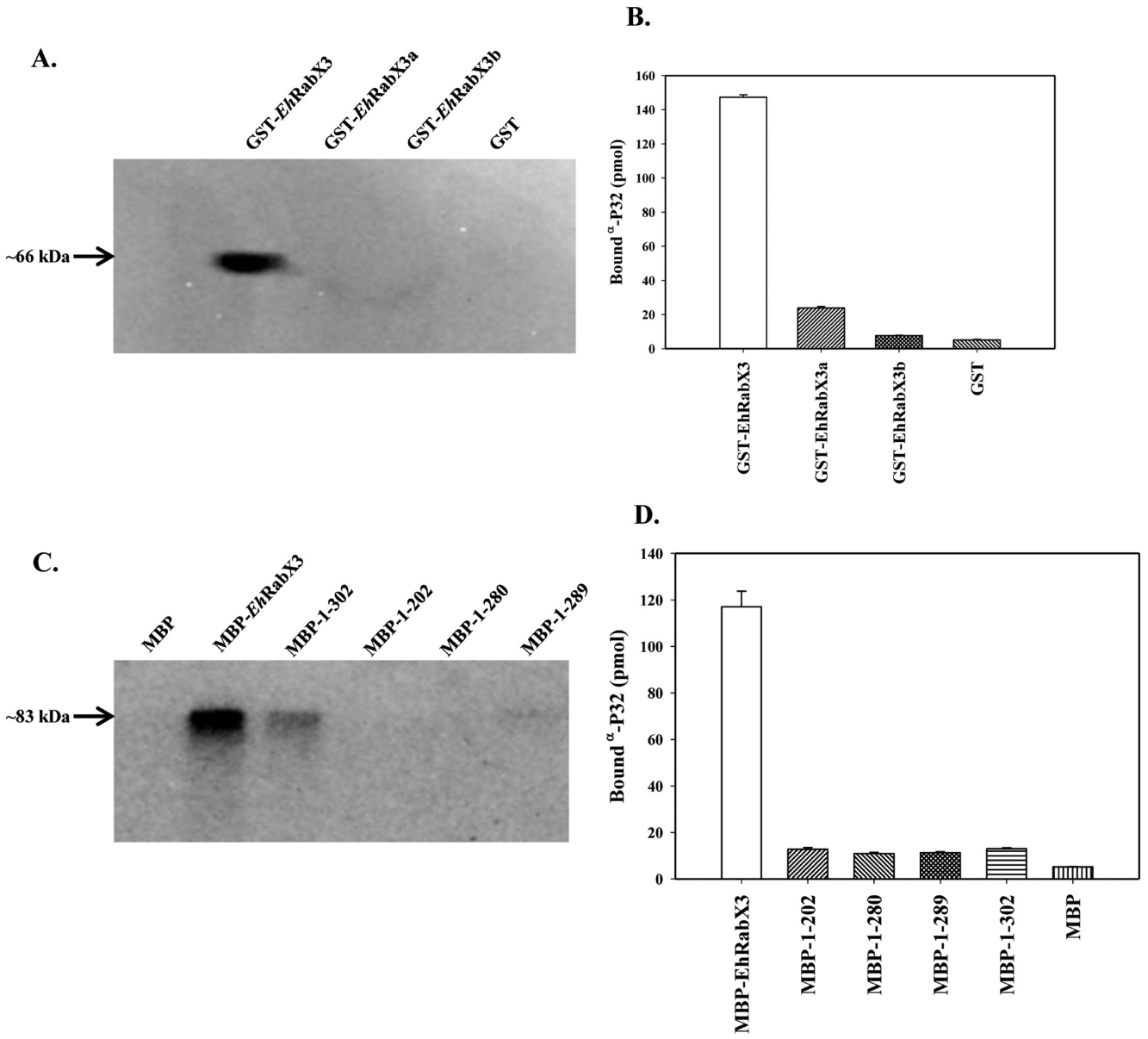

Figure 4. Potential role of the CTD of *Eh*RabX3 in nucleotide binding. *Eh*RabX3-NTD (amino acids 1−176) at 2 μM, the CTD (amino acids 177−349) at 2 μM, or C-terminal truncation constructs (amino acids 1−202, 1−280, 1−289, and 1−302) at 2 μM were incubated with 200 μM [α-^{32}P]GTP (200 μM) at 25 °C with buffer A. After 1.5 h, 20 μL aliquots were removed from each sample for SDS−PAGE analysis with an autoradiograph (A and C), and 50 μL aliquots were used for the filter binding assay (B and D). The data represent the average of three independent experiments with the negative control of GST and MBP.

nucleotide-free *Eh*RabX3. Time courses of fluorescence change (Figure 5D) were fit to an exponential growth model, yielding pseudo-first-order rate constants, k_{obs}, which depended linearly on *Eh*RabX3 concentration (Figure 5E) and were compatible with a one-step binding mechanism, represented by

$$\textit{Eh}\text{RabX3} + \text{MANT-GTP} \underset{k_{on}}{\overset{k_{off}}{\leftrightarrow}} \textit{Eh}\text{RabX3}{-}\text{MANT-GTP}$$

Association and dissociation rate constants, k_{on} and k_{off}, respectively, can be determined from the linear dependence of k_{obs} on *Eh*RabX3 concentration

$$k_{obs} = k_{on}[\textit{Eh}\text{RabX3}] + k_{off}$$

The slope of the straight line fit to the data points defines the association rate constant, k_{on} (M^{-1} s^{-1}), and the intercept with the *y*-axis yields the dissociation rate constant, k_{off} (s^{-1}). The value of k_{off} was also determined more accurately in a displacement experiment in which a 100-fold molar excess of unlabeled GTP was used to displace MANT-GTP from its complex with *Eh*RabX3 as described above. From the concentration dependence of k_{obs}, the k_{on} values were found to be similar in the presence and absence of Mg^{2+}. The equilibrium dissociation constant, K_d, was calculated from the k_{on} and k_{off} values and found to be in the micromolar range (Table 3). This finding prompted us to investigate whether *Eh*RabX3 binds to Mg^{2+} ion, at all. The Mg^{2+} binding property of *Eh*RabX3 was examined by isothermal titration calorimetry. The calorimetric data fit well to a single-set-of-sites model showing 1:1 stoichiometry (Figure S5 and Table 2 of the Supporting Information), indicating that although Mg^{2+} binds to *Eh*RabX3 it does not alter the latter's affinity for the guanine

dx.doi.org/10.1021/bi401428f | *Biochemistry* 2014, 53, 1191−1205

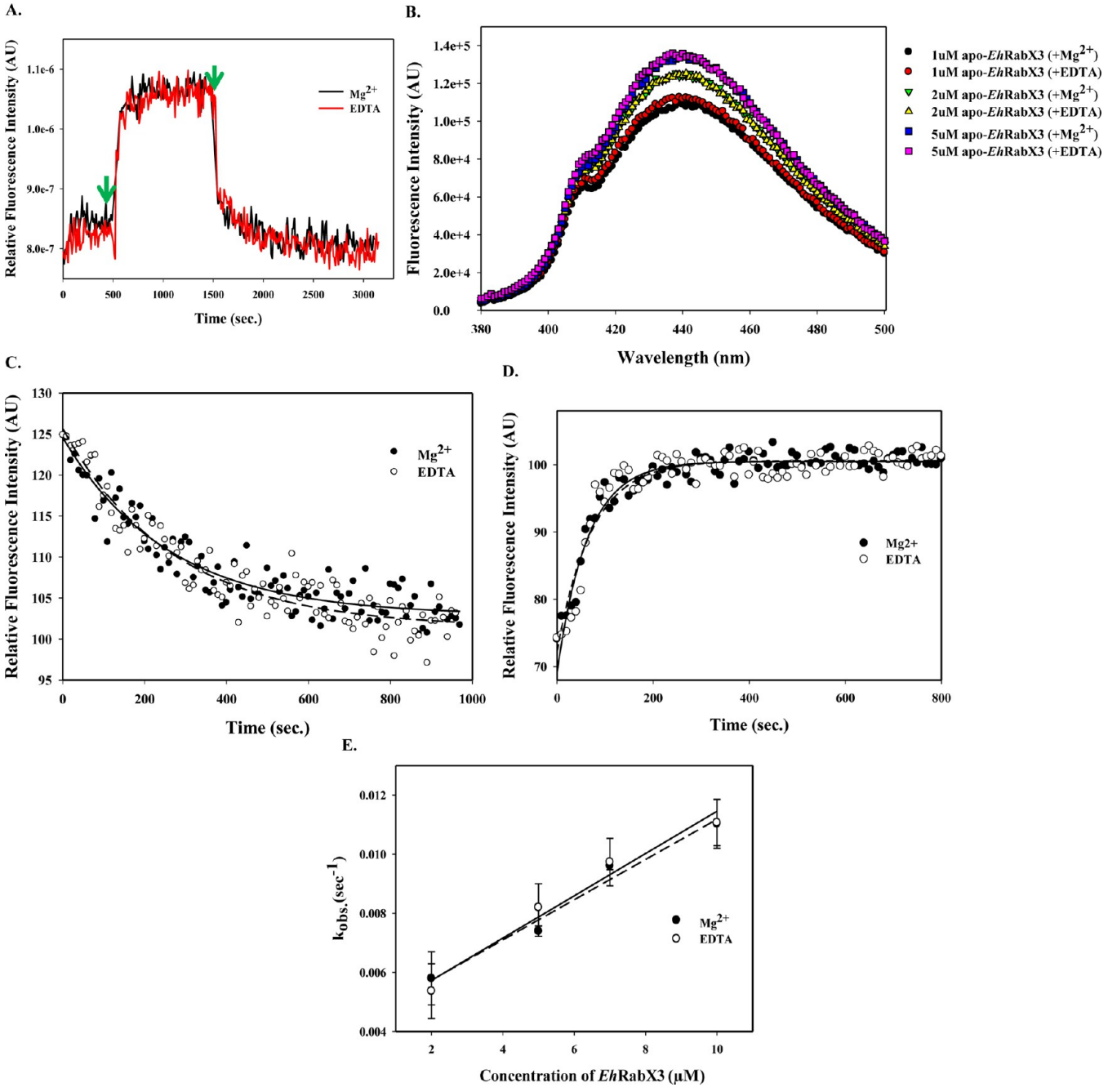

Figure 5. *Eh*RabX3 displays Mg^{2+}-independent guanine nucleotide exchange activity. Fluorescence titration measurement of *Eh*RabX3 with MANT-GTP. (A) After the baseline had been set with 350 nM MANT-GTP in buffer A containing either 5 mM $MgCl_2$ or 5 mM EDTA, 2 μM *Eh*RabX3 was added to MANT-GTP-containing buffer at the indicated time (marked by an arrowhead) and the enhancement of the fluorescence intensity was monitored. Upon saturation, excess unlabeled GTP (200 μM) was added (marked by an arrowhead) to dissociate bound MANT-GTP from *Eh*RabX3. (B) Fluorescence emission spectra of MANT-GTP (350 nM)-bound apo-*Eh*RabX3 (1, 2, and 5 μM) in buffer A containing either 5 mM $MgCl_2$ or 5 mM EDTA. After 1 h, the fluorescence emission spectra (380−500 nm) were recorded with an excitation wavelength set at 360 nm and a 4 nm emission resolution. (C) Kinetics of dissociation of MANT-GTP from *Eh*RabX3 in the presence and absence of $MgCl_2$. Time course of dissociation of MANT-GTP (350 nM) from *Eh*RabX3 (2 μM) using excess unlabeled GTP (200 μM) in buffer A containing either 5 mM $MgCl_2$ or 5 mM EDTA, as shown by monitoring the reduction in the fluorescence emission. Each data point is an average of three different measurements. Data were fit to a single-exponential decay mode to derive the apparent dissociation rate constants (k_{off}) as shown in Table 3. (D) Comparison of the association kinetics of *Eh*RabX3 with MANT-GTP in the presence and absence of $MgCl_2$. Exemplar time course for association of *Eh*RabX3 (2 μM) with 350 nM MANT-GTP in buffer A containing either 5 mM $MgCl_2$ or 5 mM EDTA, as shown by an increase in the MANT-GTP fluorescence. (E) Observed rate constants for nucleotide exchange of *Eh*RabX3 as a function of *Eh*RabX3 concentration. The observed rate constants of association (k_{obs}) from the average of three independent measurements were plotted as a function of *Eh*RabX3 concentration. k_{on} rates were derived from the slope of the linear fit to the data.

nucleotide. The binding of Mg^{2+} to *Eh*RabX3 was also found to be enthalpically controlled.

***Eh*RabX3 Is an Extremely Sluggish GTPase.** Measurement of intrinsic GTP hydrolysis is crucial to understanding the

dx.doi.org/10.1021/bi401428f | *Biochemistry* 2014, 53, 1191−1205

Table 3. Summary of Mg^{2+}-Independent Association and Dissociation Kinetics of MANT-GTP with *Eh*RabX3[a]

*Eh*RabX3	with Mg^{2+}	with EDTA
k_{off} (s^{-1})	$(4.1 \pm 0.5) \times 10^{-3}$	$(3.5 \pm 0.2) \times 10^{-3}$
k_{on} (M^{-1} s^{-1})	$(6.9 \pm 0.6) \times 10^{2}$	$(6.23 \pm 0.8) \times 10^{2}$
K_d (M)	$(5.9 \pm 0.8) \times 10^{-6}$	$(5.6 \pm 0.2) \times 10^{-6}$

[a]The dissociation constants were obtained by adding excess (100-fold) unlabeled GTP to the *Eh*RabX3−MANT-GTP complex in the presence of either 5 mM $MgCl_2$ or 5 mM EDTA as shown in Figure 4C. Data were fit to a single-exponential decay function to derive the apparent dissociation rate constants (k_{off}). For association kinetics, a constant concentration of MANT-GTP was incubated with increasing concentrations of apo-*Eh*RabX3. k_{obs} values obtained for each protein concentration were plotted as a function of protein concentration as shown in Figure 4E. k_{on} was obtained from the slope of the curve. Each value represents the results of three independent experiments.

biochemical function of a GTPase. A careful look into the HPLC profile of wild-type *Eh*RabX3 revealed a significant pool (20%) of the protein to be bound to GTP (Figure 3D), indicating a rather weak GTPase activity. To quantify the catalytic efficiency of the protein, we set out to measure the intrinsic GTPase activity of *Eh*RabX3 using a single-turnover γ-^{32}P release assay.[22−24]The detailed methodology is provided in Experimental Procedures. We found that *Eh*RabX3 has very poor hydrolytic activity compared to those of other Ras superfamily GTPases. Under the experimental condition, the extent of release of P_i by *Eh*RabX3 was below the detection limit of the assay within the experimental time limit. Therefore, we followed GTP hydrolysis up to 60 h, and the rate of P_i release was fit to first-order decay kinetics (Figure 6A). The rate constants from three independent experiments are listed in Table 4. The rate constant was found to be on the order of 10^{-5} s^{-1} and is significantly lower than that for Ras and Rab5 (rate constant on the order of 10^{-4} s^{-1}).[40] To understand the molecular basis for inefficient hydrolytic activity, we looked into the multiple-sequence alignment of *Eh*RabX3 with other Ras superfamily members. As shown in Figure 1B, we found two critical substitutions in the GTP binding pocket of *Eh*RabX3, V71 and K73, that could affect for the rate of GTP hydrolysis. The corresponding residues in other forms of hRas, A59 and Q61, play an instrumental role in GTP hydrolysis.[10] We therefore engineered *Eh*RabX3 to introduce alanine at position 71 and glutamine at position 73 and assayed the GTPase activities of the resultant mutants. While K73Q behaved almost like the wild-type protein (rate constant of 1.5×10^{-5} s^{-1}), V71A enhanced GTP hydrolysis by 7−8-fold (rate constant of 1.3×10^{-4} s^{-1}). The double mutant, V71A/K73Q, boosted the GTPase activity to a level almost equivalent to the level of those of other Ras superfamily GTPases (rate constant of 2.3×10^{-4} s^{-1}) (Figure 6B and Table 4).[8,41] This result was also confirmed by an HPLC-based intrinsic GTPase assay (Figure S6 and Table 3 of the Supporting Information).

***Eh*RabX3 Is a Cytosolic GTPase.** The GDP/GTP cycling of small GTPases is regulated by specific sets of GEFs and GAPs, which in turn regulates the localization of GTPases in distinct membrane-bound compartments. Prenylation is a prerequisite for membrane localization of a majority of Ras superfamily GTPases.[42] Interestingly, *Eh*RabX3 lacks the prenylation motif at its C-terminus and therefore is likely to localize in the amoebic cytosol. We investigated the subcellular localization of the GTPase. HA-*Eh*RabX3 was expressed in amoebic trophozoites and subjected to immunofluorescence using the anti-HA antibody. As shown in Figure 7A, 30% amoebic trophozoites showed HA staining, diffused throughout the cytoplasm. To complement the immunofluorescence result, *Eh*RabX3-expressing trophozoites were subjected to subcellular fractionation. HA-*Eh*RabX3 was probed with the anti-HA antibody on the nitrocellulose membrane, which revealed a specific band of 41 kDa (Figure 7C), indicating that HA-*Eh*RabX3 was localized in the cytosolic fraction.

DISCUSSION

*Eh*RabX3 was identified in an *in silico* screening for small GTPases in the amoebic genome.[4] The pesence of tandem GTPase domains drew our interest to investigating GTP binding and the hydrolytic property of *Eh*RabX3, including the contribution of the individual domains. *Eh*RabX3 is the only member in the eukaryotic Ras superfamily with tandem GTPase domains. The other proteins that possess double GTPase domains are EngA, a distinctive member of the Era subfamily of GTPases, and its homologue, Der. Both bacterial GTPases are involved in ribosome assembly.[7] There are multiple EngA members present in eukaryotes, including multiple protozoa. As shown in Figure S1 of the Supporting Information, the GTPase domains of *Eh*RabX3 are distinctly different from those of the EngA proteins. Unlike those of *Eh*RabX3, the individual GTPase domains of the EngA family of proteins were found to be fully capable of binding and hydrolyzing GTP.

Unlike its prokaryotic counterpart that binds to GTP with a 1:2 stoichiometry,[43] *Eh*RabX3 binds to only one molecule of GTP through its N-terminal GTPase domain as revealed by ITC. The ITC data also provided insight into the contribution of enthalpic and entropic factors underlying the interaction of the nucleotide with *Eh*RabX3. The enthalpically driven binding of GDP/GTP to *Eh*RabX3, with a negative entropic contribution, indicates the importance of H-bonding interactions and van der Waals interaction over hydrophobic interactions. The negative sign of the entropy also suggests a certain degree of order as a result of binding. Analysis of the enthalpic and entropic contributions to the free energy of binding suggests the entropic contribution is greater in GTP than in GDP, suggesting conformational changes following binding to be more in the GTP-bound form. The CTD of *Eh*RabX3 possesses an altered NKXD motif, which is critical for nucleotide discrimination. Several GTPases have been demonstrated to have significant ATPase activity because of the divergence or loss of the NKXD motif.[34] In the TRAFAC class of proteins, the GTPase activity was replaced by ATPase activity because of the deletion of the NKXD-containing region, while the SIMIBI class shows a GTP to ATP shift through divergence in the NKXD motif.[34] Therefore, we assessed the nucleotide specificity of *Eh*RabX3 using ITC and a real-time fluorescence-based binding assay. The data indicated that neither nucleotide-bound *Eh*RabX3 nor apo-*Eh*RabX3 showed any detectable binding to ATP (Figure S7A−C of the Supporting Information).

The nucleotide binding activity of the N-terminal domain was also supported by the fact that the T34N mutation in *Eh*RabX3 drastically reduced the affinity for GTP/GDP while T194N mutation, the equivalent position in the CTD, marginally altered the affinity for the nucleotides. Structural studies of hRas with a similar mutation (S17N) have shown an indispensible role of S17 in nucleotide binding. S17N reduces the affinity for GTP by 500-fold and thus favors the GDP-

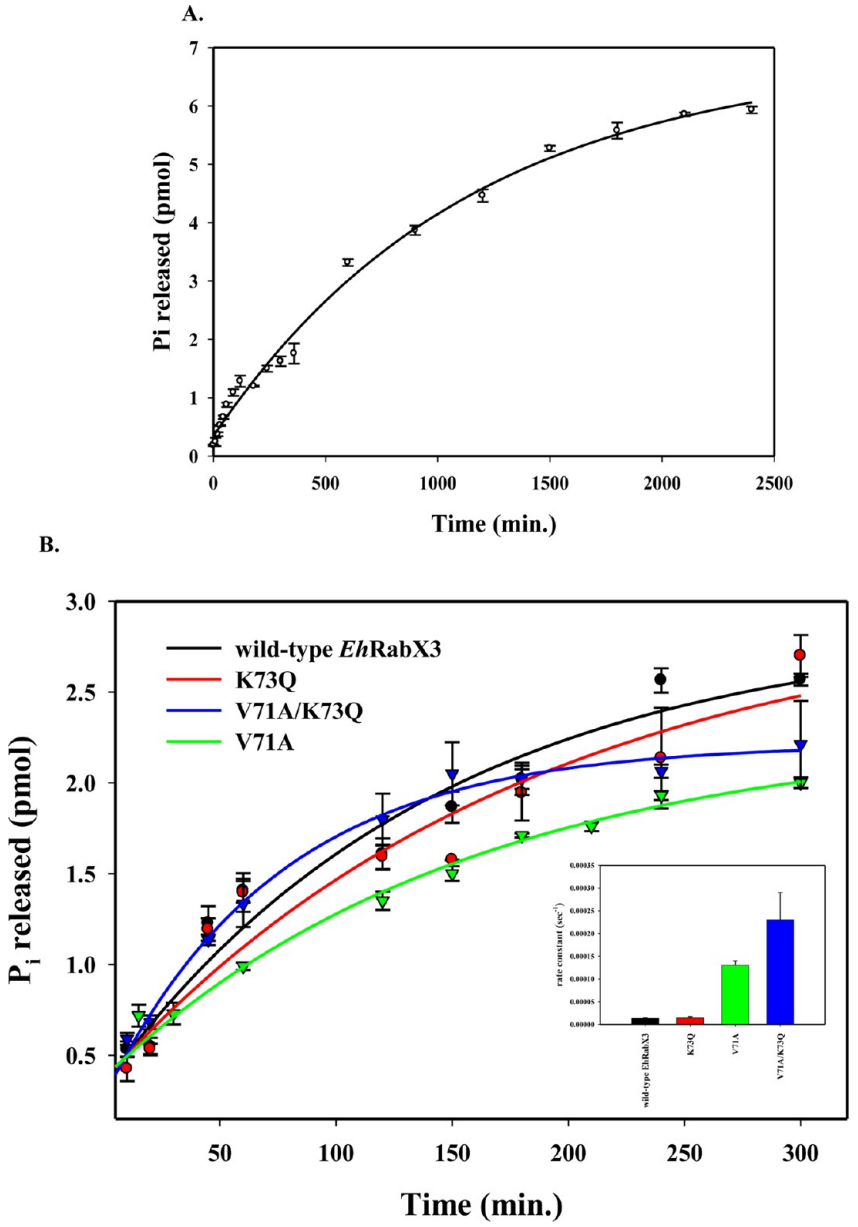

Figure 6. Extremely sluggish GTPase activity of *Eh*RabX3 and enhancement of GTPase activity by specific amino acid substitutions. A total of 200 μM wild-type (A) and mutants (B) was incubated with [γ-^{32}P]GTP (10 μCi/μL) in buffer A containing 10 mM EDTA and 2 mM unlabeled GTP at room temperature for 1.5 h. The reaction mixture was subsequently passed through a NAP-5 column and eluted in 500 μL of assay buffer. The hydrolysis was initiated by adding $MgCl_2$ to a final concentration of 20 mM. Eluted samples (15 μL) were taken at different time points (as indicated) and added to a precooled 5% charcoal solution in 50 mM NaH_2PO_4. [^{32}P]P_i in the supernatant was analyzed by scintillation counting. Data for wild-type *Eh*RabX3 and mutants (K73Q, V71A, and V71A/K73Q) are shown with different colors . The inset shows the rate constants. Each data point represents the average of three independent experiments. The values of rate constants are listed in Table 4.

bound form.[44,45] Our data suggest that the C-terminal GTPase domain of *Eh*RabX3 does not bind to the nucleotide. It could be due to the absence of two obligatory sequence motifs, NKXD and DXXG. Though our *in vitro* studies revealed that the C-terminal G-domain of *Eh*RabX3 did not show detectable binding to the guanine nucleotide, the existence of a phosphate binding site cannot be ruled out, which might have a regulatory implication in a physiological context. It is also possible that binding of an other cellular factor(s) or a post-translational modification might cause binding of a second nucleotide to the C-terminal G-domain. Alternatively, it might also be involved in maintaining the three-dimensional architecture of the GTP binding site in the NTD.

The nucleotide binding affinities of various Ras superfamily proteins vary from picomolar to nanomolar.[44,46] *Eh*RabX3 binds to guanine nucleotides with an affinity in the micromolar range that is unaltered by the presence or absence of the Mg^{2+} ion. The relatively weaker affinity of *Eh*RabX3 might be attributed to lack of some of the essential amino acids that are conserved in the other superfamily members. As shown in Figure 1B, both N- and C-terminal GTPase domains of *Eh*RabX3 lack the switch I motif.[4] This motif is known to show a change in conformation upon nucleotide binding. Additionally, *Eh*RabX3 lacks a conserved phenylalanine at position 45 (F28 in Ras and Rac1) (Figure 1B). F28 has been shown to stabilize the guanine base of GDP and GTP nucleotides

dx.doi.org/10.1021/bi401428f | *Biochemistry* 2014, 53, 1191−1205

Table 4. Intrinsic GTPase Rate Constants of Wild-Type *Eh*RabX3 and Various Mutants (K73Q, V71A, and V71A/K73Q)[a]

protein	rate of GTP hydrolysis (s^{-1})
wild-type *Eh*RabX3	$(1.4 \pm 0.1) \times 10^{-5}$
K73Q	$(1.5 \pm 0.2) \times 10^{-5}$
V71A	$(1.3 \pm 0.1) \times 10^{-4}$
V71A/K73Q	$(2.3 \pm 0.6) \times 10^{-4}$

[a]The results of the intrinsic GTPase assay as shown in Figure 6 were analyzed by fitting each data point to a single-exponential function, which yielded the rate constant for intrinsic GTP hydrolysis for each recombinant protein. Results are representative of three independent experiments.

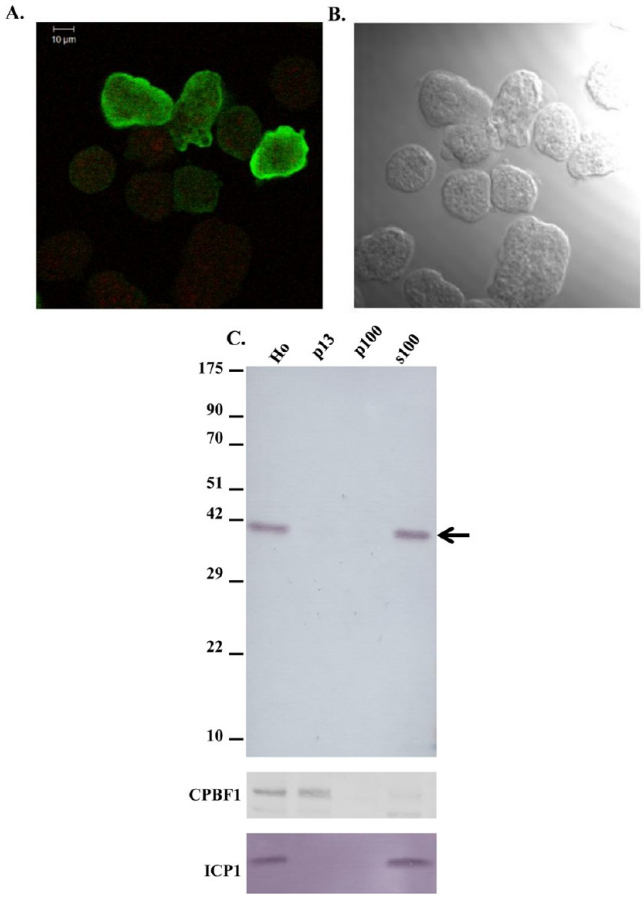

Figure 7. *Eh*RabX3 is a cytosolic GTPase. (A) Indirect immunofluorescence assay of HA-*Eh*RabX3 expressing amoeba trophozoites. HA-*Eh*RabX3 transformant cells were subjected to the immunofluorescence assay using the anti-HA antibody and imaged via (A) confocal microscopy and (B) differential interference contrast (DIC). (C) Subcellular fractionation of HA-*Eh*RabX3. The amoebic total homogenate was separated into low-speed pellet (p13), high-speed pellet (p100), and supernatant (s100) fractions, and these fractions were subjected to immunoblot analyses using the anti-HA antibody to probe HA-*Eh*RabX3 (as indicated by an arrowhead). CPBF1 (membrane marker) and ICP1 (cytosolic marker) were probed with anti-CPBF1 and anti-ICP1 antibodies, respectively.

through hydrophobic interactions. Substitution of F28 with leucine results in the spontaneous activation of Rac1, causing a "fast-cycling" phenotype.[47] In other Rho family GTPases, the F28L mutation results in a reduced affinity for the nucleotide.[48,49] The lack of phenylalanine at this position in *Eh*RabX3 might result in the reduction of the nucleotide binding affinity for this GTPase. In addition, *Eh*RabX3 possesses an altered G5 motif with Ala replaced with Thr at position 158 (Figure 1B). In Ras superfamily members, the backbone amide group at this position participates in the H-bonding interaction with the exocyclic keto group of the guanine base and is thereby known to assist in nucleotide binding.[50,51] To determine whether the altered G5 motif contributes to the weaker affinity and/or specificity for the guanine nucleotide, we analyzed the three-dimensional disposition of the motif in the homology model of the NTD of *Eh*RabX3 (Figure 8A,B). The model was built using human Rab4a [Protein Data Bank (PDB) entry 1YU9][52] as the template (see the methods in the Supporting Information). Our analysis revealed that T158 in *Eh*RabX3 retained the H-bond interaction between its amide nitrogen and the exocyclic keto oxygen from the guanine base as seen in the case of other Ras superfamily GTPases. Moreover, the fact that the side chain of this residue is pointing away from the guanine base indicates that it would not likely influence the main chain H-bond interaction. Therefore, we speculate that the substitution in the G5 motif in *Eh*RabX3 is less likely to alter its affinity for the guanine nucleotide. Furthermore, our results from the calorimetric and fluorescence-based nucleotide binding experiments indicated that the replacement of Ala with Thr did not alter the nucleotide specificity of *Eh*RabX3 (Figure S7A–C of the Supporting Information).

The rate of nucleotide exchange for a majority of the Ras superfamily GTPases shows a strong Mg^{2+} dependence. The divalent cataion has been suggested to function as a GDP dissociation inhibitor.[53] High-resolution crystal structures of Ras superfamily proteins have revealed that the cation is an integral part of the GTP binding pocket.[50,54] The protein-bound cation is known to be stabilized by (a) a conserved serine or threonine residue from the switch I region, (b) a conserved aspartic acid from switch II through water-mediated interactions, and (c) a conserved serine or threonine from the P-loop region. The lack of a switch I region in *Eh*RabX3 (Figures 1A,B and 8A,B) is likely to alter the overall integrity of the nucleotide binding pocket. In addition, substitution of conserved catalytic glutamine by lysine introduced additional positive charge into the binding pocket of *Eh*RabX3, thereby altering the overall electrostatic property of the binding site. Collectively, our results suggest that *Eh*RabX3 might have a unique nucleotide binding site.

The biological activities of the GTPases are executed by their GTP-bound forms. The rate of GTP hydrolysis determines the lifetime of the active population of a GTPase. Thus, measurement of the intrinsic GTP hydrolysis is an important step for understanding the function of a GTPase. *Eh*RabX3 is one of the most sluggish members of the Ras superfamily.[8,41] The primary sequence alignment of *Eh*RabX3 with other small GTPases revealed two critical substitutions in the switch II region, at residues V71 and K73 (Figure 1B). In human Ras, the equivalent residues, A59 and Q61, respectively, play a catalytic role in the hydrolysis reaction as revealed by crystal structure analysis and molecular dynamics simulation.[55−57] Substitution of any of these residues completely abolishes the GTPase activity of Ras. The detailed mechanism of GTP hydrolysis for Rab family GTPases is unknown, and therefore, the exact role of V71 or K73 in the catalysis is not clear. In the study presented here, while V71A improved the GTP hydrolysis rate by almost 7−8-fold, the K73Q mutant did not

dx.doi.org/10.1021/bi401428f | *Biochemistry* 2014, 53, 1191−1205

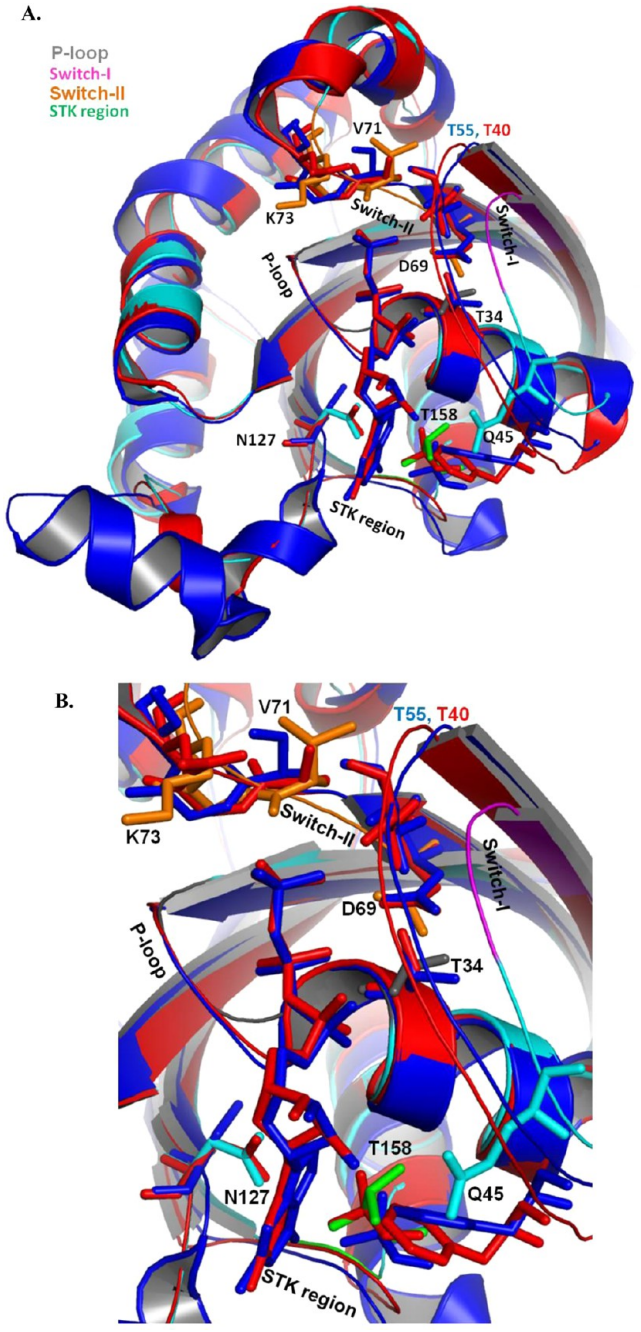

Figure 8. Implication of critical residues involved in nucleotide binding and hydrolysis by *Eh*RabX3. (A) Global view and (B) close-up view of the structural superposition of the nucleotide binding site of the homology-modeled *Eh*RabX3 (cyan) on the GNP-bound Rab4a (red) (PDB entry 1YU9) and GTP-bound Rnd3/RhoE (blue) (PDB entry 1M7B).[58] The critical residues involved in nucleotide binding and hydrolysis are shown as sticks. Residues T34, Q45, D69, V71, G72, K73, and N127 in *Eh*RabX3 are labeled, which correspond to residues S22, F33, D63, A65, G66, Q67, and N121 in Rab4a and T37, F48, D77, S79, G80, S81, and C135 in Rnd3/RhoE, respectively. Switch I-specific T40 and T55 in Rab4a and RhoE, respectively (colored blue and red, respectively), are absent in *Eh*RabX3. T158 of the STK region within *Eh*RabX3, which corresponds to A152 and A179 within the G5 motif of Rab4a and RhoE, respectively, is shown in the model.

show any enhancement. The double mutant, V71A/K73Q, boosted the GTPase activity up to 20-fold. Thus, the conserved glutamine and alanine collectively influence the catalysis rate. It further suggests that alanine at position 71 is a prerequisite for the formation of a catalytically active conformation of *Eh*RabX3, which is further accelerated by the glutamine.

To understand the molecular basis of the low catalytic efficiency of *Eh*RabX3, we analyzed the three-dimensional architecture of the nucleotide binding site in the homology model of *Eh*RabX3 (Figure 8A,B). Superposition of the nucleotide binding site of *Eh*RabX3 on that of Rab4a revealed an apparent reduction in the volume of the binding pocket. The bulky hydrophobic side chain of V71 is also likely to restrict the flexibility of the switch II region, thereby inhibiting the conformational change accompanying GTP hydrolysis. The side chain of K73 is pointing away from the γ-phosphate and thus may not able to align the nucleophilic water molecule in line with the γ-phosphate, which is a prerequisite for decreasing the energy of the transition state and thus the release of γ-phosphate.[57] Our structure-based explanation is consistent with observations made for few other small GTPases that contain identical substitutions and displayed very low GTPase activity. Human RhoE, a member of the Rho family of GTPases, possesses S64 and S66 in place of V71 and K73, respectively (A59 and Q61, respectively, for Ras) (Figure 8A,B), and the structural study suggested that S64 prevents the progression to a transition state by forming a hydrogen bond with the active site waters and thus restrain them in the ground state, thus causing the GTPase to be defective. Substitution of S64 and S66 residues with their Ras counterparts improved the GTPase activity of RhoE,[8,58,59] which is consistent with our findings for *Eh*RabX3.

The cellular activities of Ras superfamily members depend on their subcellular localization. Many of the Ras superfamily members are peripheral membrane proteins. These proteins harbor a C-terminal prenylation motif that is a target of farnesylating or geranylgeranylating enzymes. *Eh*RabX3, unlike other Rab proteins, lacks the prenylation motif and is therefore detected in the soluble fraction in amoebic trophozoites. There are some Ras superfamily members that do not appear to be modified by lipids but still associate with membranes (e.g., Rit, RhoBTB, Miro, and Sar1), and a few others (e.g., Ran and Rerg) are not lipid-modified and are not bound to membranes.[60] The physiological significance of the cytosolic localization of *Eh*RabX3 needs to be functionally investigated further.

Collectively, *Eh*RabX3 is a unique ancient GTPase that over the course of evolution lost its catalytic efficiency. Perhaps association with the GTP molecule helps it to attain the necessary conformation for its biological function. It also suggests that strong selective pressure was required to yield this unique GTPase in which the GTP-bound state is predominantly favored. Thus, unlike other family members, *Eh*RabX3 might not function as a molecular switch. Our preliminary functional studies indicated its involvement in the secretion of the cysteine protease by the amoeba. Further functional studies are currently ongoing in our laboratory. We are also in the process of determining the X-ray crystal structure of *Eh*RabX3, which will help us to explain some of the unique biochemical properties of this atypical GTPase.

■ ASSOCIATED CONTENT

Supporting Information

Experimental details, legends to tables and figures, supplementary Tables 1−3, and supplementary Figures S1−S7. This

dx.doi.org/10.1021/bi401428f | *Biochemistry* 2014, 53, 1191−1205

material is available free of charge via the Internet at http://pubs.acs.org.

AUTHOR INFORMATION

Corresponding Author

*E-mail: sunando@iiserb.ac.in.

Funding

This work was supported by The Japan Society for the Promotion of Science (JSPS) and the Japan-India Science Cooperative Program (JSPS-DST) under the Joint Research Projects (13039221-000423), Grants-in-aid for Scientific Research (24590514) from the Ministry of Education, Culture, Sports, Science, and Technology of Japan, and the Department of Science and Technology of India (SERB/F/1648/2012-13).

Notes

The authors declare no competing financial interest.

ACKNOWLEDGMENTS

We thank Dr. Rajesh Kumar Murarka of the Department of Chemical Sciences and Chaithanya Kotyada, Junior Research Fellow, of the Department of Biological Sciences of Indian Institute of Science Education and Research Bhopal for helpful discussions.

ABBREVIATIONS

MANT, 2′/3′-*O*-(*N*′-methylanthraniloyl); GDP, guanosine diphosphate; GTP, guanosine triphosphate; AMPPNP, adenylyl-imidodiphosphate; Ni-NTA, nickel-nitrilotriacetic acid; GST, glutathione *S*-transferase; MBP, maltose binding protein; ITC, isothermal titration calorimetry; HPLC, high-performance liquid chromatography; k_{on}, association rate constant; k_{off}, dissociation rate constant; k_{obs}, observed rate constant; K_d, dissociation equilibrium constant.

REFERENCES

(1) Sprang, S. R. (1997) G protein mechanisms: Insights from structural analysis. *Annu. Rev. Biochem. 66*, 639−678.

(2) Vetter, I. R., and Wittinghofer, A. (2001) The guanine nucleotide-binding switch in three dimensions. *Science 294*, 1299−1304.

(3) World Health Organization (2012) Pneumococcal vaccines WHO position paper—2012—recommendations. *Vaccine 30*, 4717−4718.

(4) Saito-Nakano, Y., Loftus, B. J., Hall, N., and Nozaki, T. (2005) The diversity of Rab GTPases in *Entamoeba histolytica*. *Exp. Parasitol. 110*, 244−252.

(5) Saito-Nakano, Y., Nakazawa, M., Shigeta, Y., Takeuchi, T., and Nozaki, T. (2001) Identification and characterization of genes encoding novel Rab proteins from *Entamoeba histolytica*. *Mol. Biochem. Parasitol. 116*, 219−222.

(6) Kumagai, M., Makioka, A., Takeuchi, T., and Nozaki, T. (2004) Molecular cloning and characterization of a protein farnesyltransferase from the enteric protozoan parasite *Entamoeba histolytica*. *J. Biol. Chem. 279*, 2316−2323.

(7) Robinson, V. L., Hwang, J., Fox, E., Inouye, M., and Stock, A. M. (2002) Domain arrangement of Der, a switch protein containing two GTPase domains. *Structure 10*, 1649−1658.

(8) Foster, R., Hu, K. Q., Lu, Y., Nolan, K. M., Thissen, J., and Settleman, J. (1996) Identification of a novel human Rho protein with unusual properties: GTPase deficiency and in vivo farnesylation. *Mol. Cell. Biol. 16*, 2689−2699.

(9) Der, C. J., Finkel, T., and Cooper, G. M. (1986) Biological and biochemical properties of human rasH genes mutated at codon 61. *Cell 44*, 167−176.

(10) Feig, L. A., and Cooper, G. M. (1988) Relationship among guanine nucleotide exchange, GTP hydrolysis, and transforming potential of mutated ras proteins. *Mol. Cell. Biol. 8*, 2472−2478.

(11) Diamond, L. S., Mattern, C. F., and Bartgis, I. L. (1972) Viruses of *Entamoeba histolytica*. I. Identification of transmissible virus-like agents. *J. Virol. 9*, 326−341.

(12) Diamond, L. S., Harlow, D. R., and Cunnick, C. C. (1978) A new medium for the axenic cultivation of *Entamoeba histolytica* and other *Entamoeba*. *Trans. R. Soc. Trop. Med. Hyg. 72*, 431−432.

(13) Nakada-Tsukui, K., Okada, H., Mitra, B. N., and Nozaki, T. (2009) Phosphatidylinositol-phosphates mediate cytoskeletal reorganization during phagocytosis via a unique modular protein consisting of RhoGEF/DH and FYVE domains in the parasitic protozoon *Entamoeba histolytica*. *Cell. Microbiol. 11*, 1471−1491.

(14) Zhang, B., Zhang, Y., Wang, Z., and Zheng, Y. (2000) The role of Mg^{2+} cofactor in the guanine nucleotide exchange and GTP hydrolysis reactions of Rho family GTP-binding proteins. *J. Biol. Chem. 275*, 25299−25307.

(15) Hauryliuk, V., Mitkevich, V. A., Draycheva, A., Tankov, S., Shyp, V., Ermakov, A., Kulikova, A. A., Makarov, A. A., and Ehrenberg, M. (2009) Thermodynamics of GTP and GDP binding to bacterial initiation factor 2 suggests two types of structural transitions. *J. Mol. Biol. 394*, 621−626.

(16) Schoebel, S., Cichy, A. L., Goody, R. S., and Itzen, A. (2011) Protein LidA from *Legionella* is a Rab GTPase supereffector. *Proc. Natl. Acad. Sci. U.S.A. 108*, 17945−17950.

(17) Delprato, A., and Lambright, D. G. (2007) Structural basis for Rab GTPase activation by VPS9 domain exchange factors. *Nat. Struct. Mol. Biol. 14*, 406−412.

(18) Sasson, Y., Navon-Perry, L., Huppert, D., and Hirsch, J. A. (2011) RGK family G-domain:GTP analog complex structures and nucleotide-binding properties. *J. Mol. Biol. 413*, 372−389.

(19) Pisareva, V. P., Pisarev, A. V., Hellen, C. U., Rodnina, M. V., and Pestova, T. V. (2006) Kinetic analysis of interaction of eukaryotic release factor 3 with guanine nucleotides. *J. Biol. Chem. 281*, 40224−40235.

(20) Majumdar, S., Ramachandran, S., and Cerione, R. A. (2006) New insights into the role of conserved, essential residues in the GTP binding/GTP hydrolytic cycle of large G proteins. *J. Biol. Chem. 281*, 9219−9226.

(21) Ahmadian, M. R., Zor, T., Vogt, D., Kabsch, W., Selinger, Z., Wittinghofer, A., and Scheffzek, K. (1999) Guanosine triphosphatase stimulation of oncogenic Ras mutants. *Proc. Natl. Acad. Sci. U.S.A. 96*, 7065−7070.

(22) Thomas, C. J., Du, X., Li, P., Wang, Y., Ross, E. M., and Sprang, S. R. (2004) Uncoupling conformational change from GTP hydrolysis in a heterotrimeric G protein α-subunit. *Proc. Natl. Acad. Sci. U.S.A. 101*, 7560−7565.

(23) Mukhopadhyay, S., and Ross, E. M. (1999) Rapid GTP binding and hydrolysis by G(q) promoted by receptor and GTPase-activating proteins. *Proc. Natl. Acad. Sci. U.S.A. 96*, 9539−9544.

(24) Shutes, A., and Der, C. J. (2005) Real-time in vitro measurement of GTP hydrolysis. *Methods 37*, 183−189.

(25) Nozaki, T., Asai, T., Sanchez, L. B., Kobayashi, S., Nakazawa, M., and Takeuchi, T. (1999) Characterization of the gene encoding serine acetyltransferase, a regulated enzyme of cysteine biosynthesis from the protist parasites *Entamoeba histolytica* and *Entamoeba dispar*. Regulation and possible function of the cysteine biosynthetic pathway in *Entamoeba*. *J. Biol. Chem. 274*, 32445−32452.

(26) Saito-Nakano, Y., Yasuda, T., Nakada-Tsukui, K., Leippe, M., and Nozaki, T. (2004) Rab5-associated vacuoles play a unique role in phagocytosis of the enteric protozoan parasite *Entamoeba histolytica*. *J. Biol. Chem. 279*, 49497−49507.

(27) Samuel, T., Okada, K., Hyer, M., Welsh, K., Zapata, J. M., and Reed, J. C. (2005) cIAP1 localizes to the nuclear compartment and modulates the cell cycle. *Cancer Res. 65*, 210−218.

(28) Furukawa, A., Nakada-Tsukui, K., and Nozaki, T. (2012) Novel transmembrane receptor involved in phagosome transport of

lysozymes and β-hexosaminidase in the enteric protozoan *Entamoeba histolytica*. *PLoS Pathog. 8*, e1002539.
(29) Penuliar, G. M., Furukawa, A., Nakada-Tsukui, K., Husain, A., Sato, D., and Nozaki, T. (2012) Transcriptional and functional analysis of trifluoromethionine resistance in *Entamoeba histolytica*. *J. Antimicrob. Chemother. 67*, 375−386.
(30) Nakada-Tsukui, K., Tsuboi, K., Furukawa, A., Yamada, Y., and Nozaki, T. (2012) A novel class of cysteine protease receptors that mediate lysosomal transport. *Cell. Microbiol. 14*, 1299−1317.
(31) Sato, D., Nakada-Tsukui, K., Okada, M., and Nozaki, T. (2006) Two cysteine protease inhibitors, EhICP1 and 2, localized in distinct compartments, negatively regulate secretion in *Entamoeba histolytica*. *FEBS Lett. 580*, 5306−5312.
(32) Nakada-Tsukui, K., Saito-Nakano, Y., Husain, A., and Nozaki, T. (2010) Conservation and function of Rab small GTPases in *Entamoeba*: Annotation of *E. invadens* Rab and its use for the understanding of *Entamoeba* biology. *Exp. Parasitol. 126*, 337−347.
(33) Pereira-Leal, J. B., and Seabra, M. C. (2000) The mammalian Rab family of small GTPases: Definition of family and subfamily sequence motifs suggests a mechanism for functional specificity in the Ras superfamily. *J. Mol. Biol. 301*, 1077−1087.
(34) Leipe, D. D., Wolf, Y. I., Koonin, E. V., and Aravind, L. (2002) Classification and evolution of P-loop GTPases and related ATPases. *J. Mol. Biol. 317*, 41−72.
(35) Bharat, A., Blanchard, J. E., and Brown, E. D. (2013) A high-throughput screen of the GTPase activity of *Escherichia coli* EngA to find an inhibitor of bacterial ribosome biogenesis. *J. Biomol. Screening 18*, 830−836.
(36) Wiseman, T., Williston, S., Brandts, J. F., and Lin, L. N. (1989) Rapid measurement of binding constants and heats of binding using a new titration calorimeter. *Anal. Biochem. 179*, 131−137.
(37) Hou, X., Hagemann, N., Schoebel, S., Blankenfeldt, W., Goody, R. S., Erdmann, K. S., and Itzen, A. (2011) A structural basis for Lowe syndrome caused by mutations in the Rab-binding domain of OCRL1. *EMBO J. 30*, 1659−1670.
(38) Wang, X., Hu, B., Zimmermann, B., and Kilimann, M. W. (2001) Rim1 and rabphilin-3 bind Rab3-GTP by composite determinants partially related through N-terminal α-helix motifs. *J. Biol. Chem. 276*, 32480−32488.
(39) Cox, A. D., and Der, C. J. (2010) Ras history: The saga continues. *Small GTPases 1*, 2−27.
(40) Simon, I., Zerial, M., and Goody, R. S. (1996) Kinetics of interaction of Rab5 and Rab7 with nucleotides and magnesium ions. *J. Biol. Chem. 271*, 20470−20478.
(41) Erdman, R. A., Shellenberger, K. E., Overmeyer, J. H., and Maltese, W. A. (2000) Rab24 is an atypical member of the Rab GTPase family. Deficient GTPase activity, GDP dissociation inhibitor interaction, and prenylation of Rab24 expressed in cultured cells. *J. Biol. Chem. 275*, 3848−3856.
(42) Barr, F. A. (2013) Review series: Rab GTPases and membrane identity: Causal or inconsequential? *J. Cell Biol. 202*, 191−199.
(43) Lamb, H. K., Thompson, P., Elliott, C., Charles, I. G., Richards, J., Lockyer, M., Watkins, N., Nichols, C., Stammers, D. K., Bagshaw, C. R., Cooper, A., and Hawkins, A. R. (2007) Functional analysis of the GTPases EngA and YhbZ encoded by *Salmonella typhimurium*. *Protein Sci. 16*, 2391−2402.
(44) John, J., Rensland, H., Schlichting, I., Vetter, I., Borasio, G. D., Goody, R. S., and Wittinghofer, A. (1993) Kinetic and structural analysis of the Mg^{2+}-binding site of the guanine nucleotide-binding protein p21H-ras. *J. Biol. Chem. 268*, 923−929.
(45) Nassar, N., Singh, K., and Garcia-Diaz, M. (2010) Structure of the dominant negative S17N mutant of Ras. *Biochemistry 49*, 1970−1974.
(46) Shapiro, A. D., Riederer, M. A., and Pfeffer, S. R. (1993) Biochemical analysis of rab9, a ras-like GTPase involved in protein transport from late endosomes to the trans Golgi network. *J. Biol. Chem. 268*, 6925−6931.
(47) Davis, M. J., Ha, B. H., Holman, E. C., Halaban, R., Schlessinger, J., and Boggon, T. J. (2013) RAC1P29S is a spontaneously activating cancer-associated GTPase. *Proc. Natl. Acad. Sci. U.S.A. 110*, 912−917.
(48) Lin, R., Bagrodia, S., Cerione, R., and Manor, D. (1997) A novel Cdc42Hs mutant induces cellular transformation. *Curr. Biol. 7*, 794−797.
(49) Wu, W. J., Lin, R., Cerione, R. A., and Manor, D. (1998) Transformation activity of Cdc42 requires a region unique to Rho-related proteins. *J. Biol. Chem. 273*, 16655−16658.
(50) Pai, E. F., Krengel, U., Petsko, G. A., Goody, R. S., Kabsch, W., and Wittinghofer, A. (1990) Refined crystal structure of the triphosphate conformation of H-ras p21 at 1.35 Å resolution: Implications for the mechanism of GTP hydrolysis. *EMBO J. 9*, 2351−2359.
(51) Tong, L., Milburn, M. V., de Vos, A. M., and Kim, S. H. (1989) Structure of ras proteins. *Science 245*, 244.
(52) Eathiraj, S., Pan, X., Ritacco, C., and Lambright, D. G. (2005) Structural basis of family-wide Rab GTPase recognition by rabenosyn-5. *Nature 436*, 415−419.
(53) Pan, J. Y., Sanford, J. C., and Wessling-Resnick, M. (1996) Influence of Mg^{2+} on the structure and function of Rab5. *J. Biol. Chem. 271*, 1322−1328.
(54) Rojas, A. M., Fuentes, G., Rausell, A., and Valencia, A. (2012) The Ras protein superfamily: Evolutionary tree and role of conserved amino acids. *J. Cell Biol. 196*, 189−201.
(55) Hall, B. E., Bar-Sagi, D., and Nassar, N. (2002) The structural basis for the transition from Ras-GTP to Ras-GDP. *Proc. Natl. Acad. Sci. U.S.A. 99*, 12138−12142.
(56) Lukman, S., Grant, B. J., Gorfe, A. A., Grant, G. H., and McCammon, J. A. (2010) The distinct conformational dynamics of K-Ras and H-Ras A59G. *PLoS Comput. Biol. 6*, No. e1000922.
(57) Martin-Garcia, F., Mendieta-Moreno, J. I., Lopez-Vinas, E., Gomez-Puertas, P., and Mendieta, J. (2012) The role of Gln61 in HRas GTP hydrolysis: A quantum mechanics/molecular mechanics study. *Biophys. J. 102*, 152−157.
(58) Garavini, H., Riento, K., Phelan, J. P., McAlister, M. S., Ridley, A. J., and Keep, N. H. (2002) Crystal structure of the core domain of RhoE/Rnd3: A constitutively activated small G protein. *Biochemistry 41*, 6303−6310.
(59) Fiegen, D., Blumenstein, L., Stege, P., Vetter, I. R., and Ahmadian, M. R. (2002) Crystal structure of Rnd3/RhoE: Functional implications. *FEBS Lett. 525*, 100−104.
(60) Wennerberg, K., Rossman, K. L., and Der, C. J. (2005) The Ras superfamily at a glance. *J. Cell Sci. 118*, 843−846.
(61) Thompson, J. D., Higgins, D. G., and Gibson, T. J. (1994) CLUSTAL W: Improving the sensitivity of progressive multiple sequence alignment through sequence weighting, position-specific gap penalties and weight matrix choice. *Nucleic Acids Res. 22*, 4673−4680.
(62) Gouet, P., Courcelle, E., Stuart, D. I., and Metoz, F. (1999) ESPript: Analysis of multiple sequence alignments in PostScript. *Bioinformatics 15*, 305−308.